ELSEVIER

Journal of Alloys and Compounds 465 (2008) 64–77

Journal of ALLOYS AND COMPOUNDS

www.elsevier.com/locate/jallcom

The Al–B–Nb–Ti system III. Thermodynamic re-evaluation of the constituent binary system Al–Ti

V.T. Witusiewicz [a,*], A.A. Bondar [b], U. Hecht [a], S. Rex [a], T.Ya. Velikanova [b]

[a] *ACCESS e.V., Intzestr. 5, D-52072 Aachen, Germany*

[b] *Frantsevich Institute for Problems of Materials Science, Krzhyzhanovsky Str. 3, 03680 Kyiv, Ukraine*

Received 17 April 2007; received in revised form 23 August 2007; accepted 15 October 2007

Available online 22 October 2007

Abstract

The thermodynamic description of the binary system Al–Ti is obtained by modelling the Gibbs energy of all individual phases using the CALPHAD approach. The model parameters have been evaluated by means of the computer optimization module PARROT, available within Thermo-Calc, taking into account recent experimental data and critically assessed information on phase equilibria and thermodynamic properties. The calculations are in close agreement with the experimental data on both phase equilibria and thermodynamics in the entire Al–Ti system.

© 2007 Elsevier B.V. All rights reserved.

Keywords: Al–Ti; Phase diagram; Thermodynamic description; CALPHAD approach

1. Introduction

As pointed out in previous parts of the work [1,2], knowledge of phase equilibria and thermodynamic properties of the Al–B–Nb–Ti system is of high technological interest because niobium containing γ(TiAl)-based alloys refined by boron additions are considered to be potential materials for both aero-engine and automotive applications. The binary Al–Ti system is the core constituent system from the above quaternary one and its thermodynamic description is crucial for the development of a reliable thermodynamic database for the γ(TiAl)-based alloys. Today several thermodynamic descriptions of the Al–Ti are available [3–10] but none of them can reflect the present status of experimental data. The critical assessments [11–14] included most recent data. The authors of Refs. [11–13] combined experimental results published by Braun and Ellner [15–17] for the alloys containing ∼60–75 at.% Al with calculated phase diagrams [8,10] and obtained quite similar versions of the phase diagram (Fig. 1a). The assessment of Schuster and Palm [14] was based on a critical evaluation of all available literature data (Fig. 1b). The main differences between the phase diagrams proposed by the authors [11–14] relate to the following points (designation of phases are presented in Table 1):

(a) the melting of β (bcc_A2) solid solution is either incongruent [11–13] (and also [4,7,8,10]) or congruent [14] (and also [3,5,6,9,18]);
(b) the A2 ↔ B2 ordering in the β (bcc_A2) phase is accepted [11,13] or neglected [14];
(c) the formation of α_2 (Ti_3Al) phase is either congruent from α (hcp_A3) [11–13] or peritectoidal from α (hcp_A3) and β (bcc_A2) [14];
(d) the Ti_3Al_5 phase is accepted as stable [11–13,15–17] or metastable [14];
(e) the range between γ(TiAl) and ε($TiAl_3$) phases at temperatures starting from somewhat lower than the η ($TiAl_2$) formation and up to melting (i.e. from 63 to 73 at.% Al and from ∼1250 to ∼1720 K [14–17]) includes either two phases $Ti_{1-x}Al_{1+x}$ and $Ti_{2+x}Al_{5-x}$ [11–13,15–17] or the phase field treated as one-dimensional anti-phase structure (1d-APS) [14].

The present paper reports on the thermodynamic description of the entire binary system Al–Ti by the CALPHAD

* Corresponding author. Tel.: +49 241 8098007; fax: +49 241 38578.
E-mail address: victor@access.rwth-aachen.de (V.T. Witusiewicz).

0925-8388/$ – see front matter © 2007 Elsevier B.V. All rights reserved.
doi:10.1016/j.jallcom.2007.10.061

Table 1
The Al–Ti phases designations, most often used in the literature, their crystal structure data [14] and models employed in the present thermodynamic description

Phase (designation)	Pearson symbol	Space group	Prototype	Struktur–Bericht designation	Model employed in the present description
(L) liquid					[Al,Ti]
α, (αTi), hcp_A3	*hP*2	$P6_3/mmc$	Mg	*A*3	$[(Al,Ti)_1:(Va)_{0.5}]$
β, (βTi), bcc_A2	*cI*2	$Im\bar{3}m$	W	*A*2	$[(Al,Ti)_1:(Va)_3]$
β_0, β′, (βTi,Al), bcc_B2	*cI*2	$Pm\bar{3}m$	CsCl	*B*2	$[(Al,Ti)_1:(Va)_3]+[(Al,Ti)_{0.5}:(Al,Ti)_{0.5}:(Va)_3]$
α_2, Ti_3Al	*hP*8	$P6_3/mmc$	Ni_3Sn	$D0_{19}$	$[(Al,Ti)_3:(Al,Ti)_1]$
γ, γTiAl, TiAl	*tP*4	*P*4/*mmm*	AuCu	$L1_0$	$[(Al\%,Ti)_1:(Al,Ti\%)_1]$
$Ti_{1-x}Al_{1+x}$	Inversed to γTiAl				–
1d-APD	Tetragonal ordered superstructures of AuCu for γTiAl (included Ti_5Al_{11} and Ti_2Al_5)				–
Ti_3Al_5	*tP*32	*P*4/*mbm*	Ti_3Al_5	–	$[(Al)_5:(Ti)_3]$
η, $TiAl_2$	*tI*24	$I4_1/amd$	$HfGa_2$	–	$[(Al,Ti)_2:(Al,Ti)_1]$
Ti_5Al_{11}	*tI*16	*I*4/*mmm*	$ZrAl_3$	$D0_{23}$	–
ζ, $Ti_{2+x}Al_{5-x}$	*tP*28	*P*4/*mmm*	Ti_2Al_5	–	$[(Al,Ti)_5:(Al,Ti)_2]$
ε(h), $TiAl_3$(HT), $TiAl_3$(h)	*tI*8	*I*4/*mmm*	$TiAl_3$(h)	$D0_{22}$	$[(Al,Ti)_3:(Al,Ti)_1]$
ε(l), $TiAl_3$(LT), $TiAl_3$(l)	*tI*32	*I*4/*mmm*	$TiAl_3$(l)	–	$[(Al,Ti)_3:(Al,Ti)_1]$
αAl, fcc_A1	*cF*4	$Fm\bar{3}m$	Cu	*A*1	$[(Al,Ti)_1:(Va)_1]$

approach, based on experimental data available, the majority of which were assessed in Ref. [14], being complemented by key experiments performed as a part of the present work (PW).

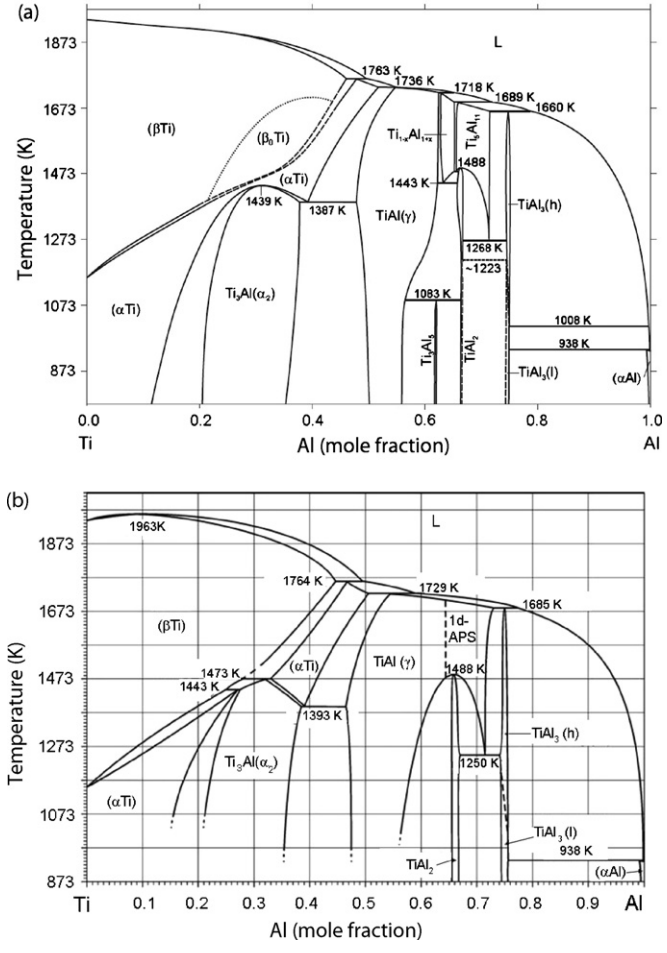

Fig. 1. The Ti–Al phase diagram according to recent critical assessments by Grytsiv et al. [11] (a) and Schuster and Palm [14] (b).

2. Experimental

In order to verify the congruent melting of the β (bcc_A2) phase as well as melting of α (hcp_A3), γ(TiAl), and ε($TiAl_3$) phases, eight alloys (Table 2) were prepared by arc melting with a non-consumable tungsten electrode on a water-cooled copper hearth under purified argon. Materials used for alloy preparation were a master alloy Ti–55 at.% Al melted from Al plates (purity 99.99 wt.% Al) and Ti obtained from the iodide titanium process with a purity of 99.9 wt.% Ti, as well as the pure metals themselves. The composition of the master alloy was checked by wet chemical analysis. The samples were prepared without essential losses in mass and were subjected to DTA. Afterwards the samples were annealed at sub-solidus temperatures for 4–10 h in Ar, gettered with Ti cuttings, using a resistance furnace. In some cases annealing was followed by quenching in liquid gallium. As shown by reducing extraction in a Ni bath followed by chromatography, the Al–Ti alloys, both in the as-cast and annealed condition, contained from 0.01 to 0.07 mass% O, while N and H contamination was lower than the sensitivity threshold of about 0.03 mass%. The DTA curves upon heating and cooling with rates of 20 and 40(or 45) K min^{-1} were obtained for the pure Ti and for each of the alloys, with the samples being contained in small scandia crucibles. The DTA apparatus was calibrated at the same heating (cooling) rates using the reference points of IPTS-90 (Al, Ag, Au, Pd, Pt, and Ru) and of high purity Fe. The calibration showed an accurate reproducibility of all transformation temperatures. The mass of the DTA samples ranged from 0.2 to 0.4 g. Some examples of the DTA curves for as-cast and annealed samples obtained at different heating and cooling rates are shown in Fig. 2a–c.

From Fig. 2a it is obvious that Ti–10.0 at.% Al melts at a temperature of 17 and 22 K higher than both, pure Ti and Ti–22.5 at.% Al, proving the existence of congruent melting of the β phase.

Table 2 contains the phase transformation temperatures detected by DTA in all the samples. From the table it is evident that the differences that may originate from processing samples in different conditions (e.g. as-cast and annealed) or at different heating and cooling rates are small, basically within experimental errors at these temperature levels. This was also confirmed by comparing the XRD patterns of as-cast and annealed samples: from the sharp reflections one can infer on the absence of severe constitutional liquation.

3. Thermodynamic models

The Gibbs energy descriptions of the stable and metastable structures of the pure elements are adopted from the SGTE database compiled by Dinsdale [19].

The 12 phases considered in the present description of the Al–Ti system are: liquid (L), α solid solution or hcp_A3, dis-

Table 2
DTA data (K) for the Ti–Al alloys in comparison with transformation temperatures calculated using present thermodynamic description

Al (at.%)	State of sample	Phase transformation	Heating (K min^{-1})		Cooling (K min^{-1})		Result	
			40/45	20	40/45	20	Recomended[a]	Calculated
10.0	As-cast (*)	$\alpha \leftrightarrow \alpha + \beta$	1278*				1278	1275
		$\alpha + \beta \leftrightarrow \beta$						1284
		$\beta \leftrightarrow L$	1962*				1962	1963
22.5	As-cast (*)	$\alpha_2 \leftrightarrow \alpha_2 + \alpha$	1253*					1204
		$\alpha_2 + \alpha \leftrightarrow \alpha$	1318*		1338		1318	1295
		$\alpha \leftrightarrow \alpha + \beta$	1387		1443		1387	1384
		$\alpha + \beta \leftrightarrow \beta$						1392
		$\beta \leftrightarrow L + \beta$	1940*				1940	1939
		$L + \beta \leftrightarrow L$	1955*		1948		1948–1955	1944
47.5	Annealed 10 h/1673 K	$\gamma \leftrightarrow \gamma + \alpha$	1500	1493	1476	1487	1487–1493	1488
		$\gamma + \alpha \leftrightarrow \alpha$	1645	1647	1595	1614	1647	1644
		$\alpha \leftrightarrow L + \alpha$	1754	1756			1756	1758
		$L + \alpha \leftrightarrow L + \beta$	1767	1761	1751	1744	1761	1764
		$L + \beta \leftrightarrow L$	1800	1796	1775	1783	1783–1796	1786
49.0	As-cast (*) and annealed 10 h/1673 K	$\gamma \leftrightarrow \gamma + \alpha$	1553*	1533	1476			1579
		$\gamma + \alpha \leftrightarrow \alpha$	1678*	1655	1788	1674	1655–1678	1678
		$\alpha \leftrightarrow L + \alpha$	1758*	1747			1747	1748
		$L + \alpha \leftrightarrow L + \beta$		1772		1757	1757–1772	1764
		$L + \beta \leftrightarrow L$	1793*	1783	1788	1768	1768–1783	1768
50.5	Annealed 10 h/1673 K	$\gamma \leftrightarrow \gamma + \alpha$		1575		1530		1627
		$\gamma + \alpha \leftrightarrow \alpha$		1704		1669	1669–1704	1709
		$\alpha \leftrightarrow L + \alpha$		1732		1702	1732	1737
		$L + \alpha \leftrightarrow L$		1771		1755	1755–1771	1757
55.0	As-cast (*)	$\gamma \leftrightarrow L + \gamma$	1723*		1713		1723	1728
		$L + \gamma \leftrightarrow L$	1753*		1723		1723	1729
73.5	As-cast (*) and annealed 4 h/1633 K/quenched in liq. Ga	$\varepsilon \leftrightarrow L + \zeta$	1683/1678*				1678	1669
		$L + \zeta \leftrightarrow L$	1728/1718*		1683/1683*		1683	1676
75.3	Annealed 5 h/1623 K	$\varepsilon(h) \leftrightarrow L + \varepsilon(h)$	1638	1614		1620	1614	1595
		$L + \varepsilon(h) \leftrightarrow L$	1683	1675		1667	1667–1675	1669

Transformation temperatures marked with (*) result from samples in the as-cast state.
[a] Recommended values are selected mainly with preference for heating curves.

ordered β solid solution or bcc_A2, ordered β_0 solid solution or bcc_B2, α_2 or Ti_3Al, γ or TiAl, Ti_3Al_5, η or $TiAl_2$, ζ or Ti_2Al_5, the low temperature modification of ε(l) or $TiAl_3$(l), the high-temperature modification of ε(h) or $TiAl_3$(h) and finally the (αAl) solid solution or fcc_A1 phase. The designations of Al–Ti phases, which are most often used in the literature, their crystal structure data and models employed in the present thermodynamic description are summarised in Table 1.

The liquid phase is modelled as substitutional solution by applying the Redlich–Kister formalism [20]. The metal solid solutions based on αAl (fcc_A1), β (bcc_A2) and α (hcp_A3) phases are modelled as disordered solution phases using the two-sublattice model where the second sublattice is occupied by vacancies. The remaining phases, excluding β_0 (bcc_B2), are treated as ordered phases by using the two-sublattice model proposed by Hillert and Staffansson [21]. It should be mentioned that the ordered α_2 (Ti_3Al) and γ(TiAl) phases and disordered phases corresponding to α (hcp_A3) and αAl (fcc_A1), respectively, are modelled by separate models, which allows a simple integration of this description into higher order databases. The β_0 (bcc_B2) is modelled by a unified three-sublattice model, which includes the contribution from disordered β (bcc_A2). The expressions for the molar Gibbs energy as function of temperature and composition for these models are mainly given in the first part of our work [1] or in Refs. [22,23].

4. Optimization

The model parameters of the phases listed above were evaluated by searching for the best fit to experimental equilibrium data [10–17,24–51] and to thermodynamic properties of alloys [52–62] using the PARROT optimizer of the computer program Thermo-Calc [22]. The PARROT module can handle various kinds of experimental data and minimise an error sum, once each of the selected experimental values is accorded a certain weight. The weight is chosen by personal judgement and may be changed during the optimization work until most of the selected experimental data are reproduced within the scatter of experimental data. It should be pointed out that during the process of optimization a 1.5 times higher weight (confidence) was accorded to the present DTA data and for the values accepted in [14] for the temperatures and the phase compositions at the invariant reactions, because the authors of [14] have performed thorough analysis of the majority of original experimental data.

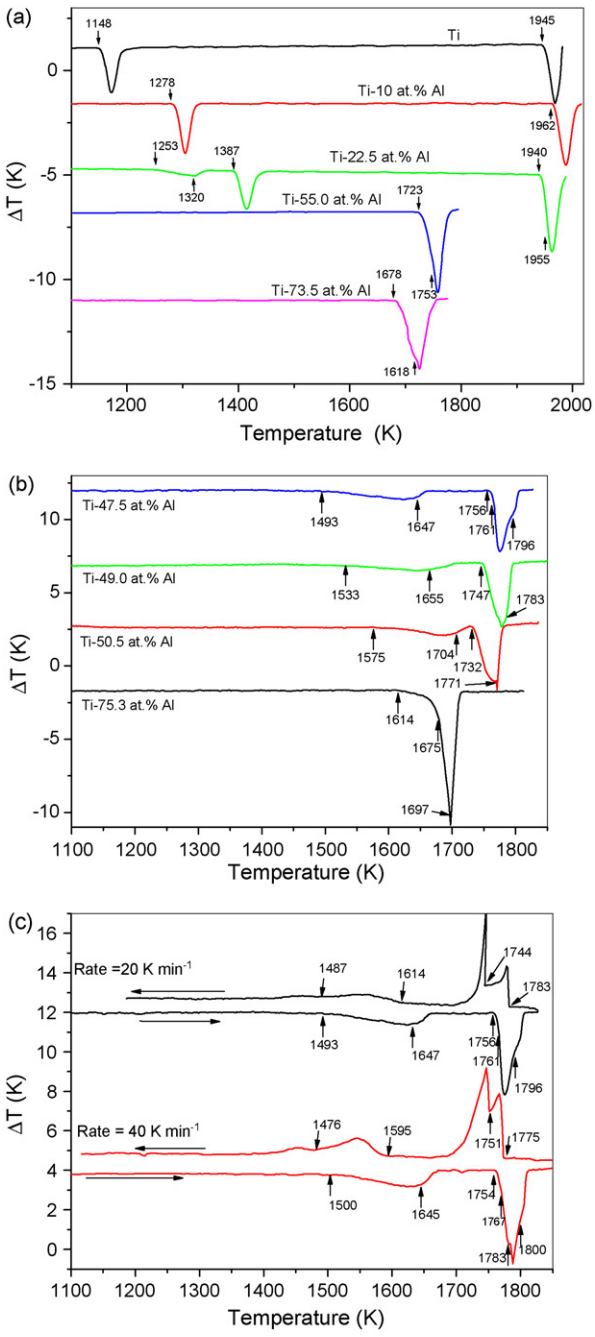

Fig. 2. Examples of the DTA curves of pure Ti and Ti–Al alloys processed in Sc_2O_3 crucibles: (a) heating curves with a rate of 45 K min^{-1} for selected as-cast samples, (b) heating curves with a rate of 20 K min^{-1} for selected samples annealed for 10 h at sub-solidus temperatures (1623–1673 K) and (c) heating and cooling curves with rates of 20 and 40 K min^{-1}, respectively for a Ti–47.5 at.% Al sample annealed for 10 h at 1673 K.

The optimization process was as follows: firstly the thermodynamic parameters of the liquid, β (bcc_A2), α (hcp_A3), αAl (fcc_A1) and ε($TiAl_3$) phases were optimized. In the second step the parameters for the ordered α_2 (Ti_3Al) and γ(TiAl), η ($TiAl_2$) were adjusted. After that the ε($TiAl_3$) was subdivided for the low temperature ε(l) ($TiAl_3$(l)) and high-temperature ε(h) ($TiAl_3$(h)) phases and the parameters for these phases were obtained. The next step was dedicated to the optimization of the thermodynamic parameters for the ζ (Ti_2Al_5) and Ti_3Al_5 phases. In the final runs it was allowed to first vary all enthalpic parameters at fixed entropic terms for all phases and then vice versa. Since the data on the enthalpy of formation of liquid and solid alloys are available and the experimental phase equilibria data cover a large temperature range, these allow us to model the enthalpic and the entropic terms for all phases independently. The ultimate set of the parameters that was evaluated for the binary system Al–Ti is presented in Table 3.

5. Results and discussion

The phase equilibria and thermodynamic properties presented in this section were calculated using the computer

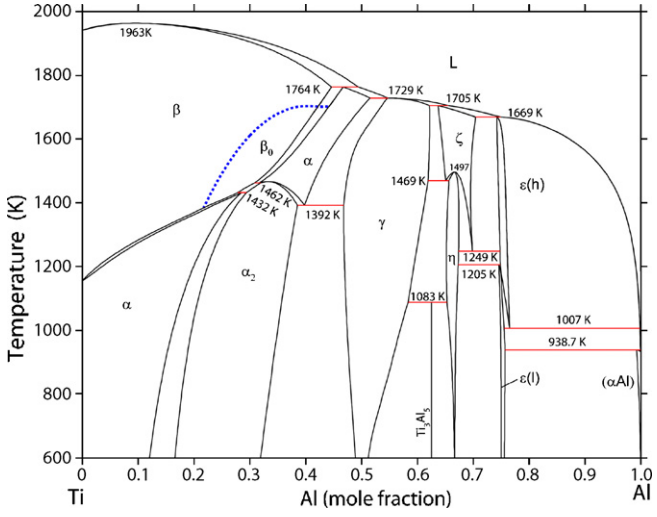

Fig. 3. The Ti–Al system according to the present thermodynamic description.

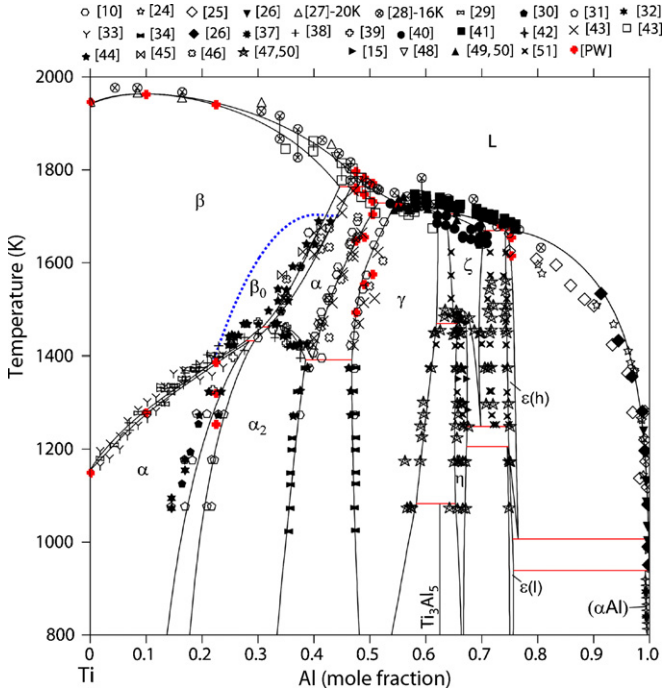

Fig. 4. Comparison of the calculated phase diagram of the Ti–Al system with experimental data of Refs. [10,15,24–51] and the present DTA data [PW].

Table 3
Summary of thermodynamic parameters for the phases in the binary system Al–Ti (all values are given in SI units (J, mol, K) and for one formula unit)

Phase	Parameters (J mol^{-1})
Liquid (L)	${}^0L^{\mathrm{Liq}}_{\mathrm{Al,Ti}} = -118048 + 41.972T$; ${}^1L^{\mathrm{Liq}}_{\mathrm{Al,Ti}} = -23613 + 19.704T$; ${}^2L^{\mathrm{Liq}}_{\mathrm{Al,Ti}} = 34757 - 13.844T$
fcc_A1 (αAl)	${}^0G^{\mathrm{fcc}}_{\mathrm{Ti:Va}} = {}^0G^{\mathrm{fcc}}_{\mathrm{Ti}}$; ${}^0G^{\mathrm{fcc}}_{\mathrm{Al:Va}} = {}^0G^{\mathrm{SER}}_{\mathrm{Al}}$; ${}^0L^{\mathrm{fcc}}_{\mathrm{Al,Ti:Va}} = -119185 + 40.723T$
hcp_A3 (α)	${}^0G^{\mathrm{hcp}}_{\mathrm{Ti:Va}} = {}^0G^{\mathrm{SER}}_{\mathrm{Ti}}$; ${}^0G^{\mathrm{hcp}}_{\mathrm{Al:Va}} = {}^0G^{\mathrm{hcp}}_{\mathrm{Al}}$; ${}^0L^{\mathrm{hcp}}_{\mathrm{Al,Ti:Va}} = -134164 + 37.863T$; ${}^1L^{\mathrm{hcp}}_{\mathrm{Al,Ti:Va}} = -3475 + 0.825T$; ${}^2L^{\mathrm{hcp}}_{\mathrm{Al,Ti:Va}} = -7756$
Ti_3Al (α_2)	${}^0G^{\mathrm{Ti_3Al}}_{\mathrm{Al:Al}} = 4{}^0G^{\mathrm{hcp}}_{\mathrm{Al}}$; ${}^0G^{\mathrm{Ti_3Al}}_{\mathrm{Ti:Ti}} = 4{}^0G^{\mathrm{SER}}_{\mathrm{Ti}} + 20$; ${}^0G^{\mathrm{Ti_3Al}}_{\mathrm{Al:Ti}} = 3{}^0G^{\mathrm{hcp}}_{\mathrm{Al}} + {}^0G^{\mathrm{SER}}_{\mathrm{Ti}} - 16443 + 5.400T$; ${}^0G^{\mathrm{Ti_3Al}}_{\mathrm{Ti:Al}} = {}^0G^{\mathrm{hcp}}_{\mathrm{Al}} + 3{}^0H^{\mathrm{SER}}_{\mathrm{Ti}} - 113676 + 20.833T$; ${}^0L^{\mathrm{Ti_3Al}}_{\mathrm{Al,Ti:Al}} = -269912 + 86.338T$; ${}^0L^{\mathrm{Ti_3Al}}_{\mathrm{Ti:Al,Ti}} = -13704 + 5.318T$
bcc_A2 (β) and bcc_B2 (β_0)	
Disordered state	${}^0G^{\mathrm{bcc\_A2}}_{\mathrm{Ti:Va}} = {}^0G^{\mathrm{bcc}}_{\mathrm{Ti}}$; ${}^0G^{\mathrm{bcc\_A2}}_{\mathrm{Al:Va}} = {}^0G^{\mathrm{bcc}}_{\mathrm{Al}}$; ${}^0L^{\mathrm{bcc\_A2}}_{\mathrm{Al,Ti:Va}} = -132903 + 39.961T$; ${}^1L^{\mathrm{bcc\_A2}}_{\mathrm{Al,Ti:Va}} = 4890$ ${}^2L^{\mathrm{bcc\_A2}}_{\mathrm{Al,Ti:Va}} = 400$
Ordering energy	${}^0L^{\mathrm{bcc\_B2}}_{\mathrm{Al:Ti:Va}} = {}^0L^{\mathrm{bcc\_B2}}_{\mathrm{Ti:Al:Va}} = -175001$; ${}^0L^{\mathrm{bcc\_B2}}_{\mathrm{Al,Ti:Al:Va}} = {}^0L^{\mathrm{bcc\_B2}}_{\mathrm{Al:Al,Ti:Va}} = 6155$; ${}^1L^{\mathrm{bcc\_B2}}_{\mathrm{Al,Ti:Al:Va}} = {}^1L^{\mathrm{bcc\_B2}}_{\mathrm{Al:Al,Ti:Va}} = 6292$; ${}^0L^{\mathrm{bcc\_B2}}_{\mathrm{Al,Ti:Ti:Va}} = {}^0L^{\mathrm{bcc\_B2}}_{\mathrm{Ti:Al,Ti:Va}} = -21406$; ${}^1L^{\mathrm{bcc\_B2}}_{\mathrm{Al,Ti:Ti:Va}} = {}^1L^{\mathrm{bcc\_B2}}_{\mathrm{Ti:Al,Ti:Va}} = -1080$
TiAl (γ)	${}^0G^{\mathrm{TiAl}}_{\mathrm{Al:Al}} = 4 + 2{}^0G^{\mathrm{SER}}_{\mathrm{Al}}$; ${}^0G^{\mathrm{TiAl}}_{\mathrm{Ti:Ti}} = 2{}^0G^{\mathrm{fcc}}_{\mathrm{Ti}}$; ${}^0G^{\mathrm{TiAl}}_{\mathrm{Al,Ti}} = {}^0G^{\mathrm{TiAl}}_{\mathrm{Ti,Al}} = {}^0G^{\mathrm{SER}}_{\mathrm{Al}} + {}^0G^{\mathrm{fcc}}_{\mathrm{Ti}} - 81008 + 14.722T$; ${}^0L^{\mathrm{TiAl}}_{\mathrm{Al,Ti:Ti}} = {}^0L^{\mathrm{TiAl}}_{\mathrm{Ti:Al,Ti}} = -31963 + 6.952T$; ${}^0L^{\mathrm{TiAl}}_{\mathrm{Al,Ti:Al}} = {}^0L^{\mathrm{TiAl}}_{\mathrm{Al:Al,Ti}} = -88993 + 41.695T$; ${}^1L^{\mathrm{TiAl}}_{\mathrm{Al,Ti:Al}} = {}^1L^{\mathrm{TiAl}}_{\mathrm{Al:Al,Ti}} = 27363$; ${}^2L^{\mathrm{TiAl}}_{\mathrm{Al,Ti:Al}} = {}^2L^{\mathrm{TiAl}}_{\mathrm{Al:Al,Ti}} = 42189$
TiAl3(h) (ε(h))	${}^0G^{\mathrm{TiAl_3(h)}}_{\mathrm{Ti:Ti}} = 80000 + 4{}^0G^{\mathrm{SER}}_{\mathrm{Ti}}$; ${}^0G^{\mathrm{TiAl_3(h)}}_{\mathrm{Al:Al}} = 80000 + 4{}^0G^{\mathrm{SER}}_{\mathrm{Al}}$; ${}^0G^{\mathrm{TiAl_3(h)}}_{\mathrm{Ti:Al}} = 3{}^0G^{\mathrm{SER}}_{\mathrm{Ti}} + {}^0G^{\mathrm{SER}}_{\mathrm{Al}} - 72097$; ${}^0G^{\mathrm{TiAl_3(h)}}_{\mathrm{Al:Ti}} = 3{}^0G^{\mathrm{SER}}_{\mathrm{Al}} + {}^0G^{\mathrm{SER}}_{\mathrm{Ti}} - 143733 + 35.088T$; ${}^0L^{\mathrm{TiAl_3(h)}}_{\mathrm{Al,Ti:Al}} = {}^0L^{\mathrm{TiAl_3(h)}}_{\mathrm{Al:Al,Ti}} = -67583$; ${}^0L^{\mathrm{TiAl_3(h)}}_{\mathrm{Al,Ti:Ti}} = {}^0L^{\mathrm{TiAl_3(h)}}_{\mathrm{Ti:Al,Ti}} = -93086$
TiAl3(l) (ε(h))	${}^0G^{\mathrm{TiAl_3(l)}}_{\mathrm{Al:Al}} = 80000 + 4{}^0G^{\mathrm{SER}}_{\mathrm{Al}}$; ${}^0G^{\mathrm{TiAl_3(l)}}_{\mathrm{Ti:Ti}} = 80000 + 4{}^0G^{\mathrm{SER}}_{\mathrm{Ti}}$; ${}^0G^{\mathrm{TiAl_3(l)}}_{\mathrm{Al:Ti}} = 3{}^0G^{\mathrm{SER}}_{\mathrm{Al}} + {}^0G^{\mathrm{SER}}_{\mathrm{Ti}} - 147620 + 38.395T$; ${}^0G^{\mathrm{TiAl_3(l)}}_{\mathrm{Ti:Al}} = 3{}^0G^{\mathrm{SER}}_{\mathrm{Ti}} + {}^0G^{\mathrm{SER}}_{\mathrm{Al}} - 53950$; ${}^0L^{\mathrm{TiAl_3(l)}}_{\mathrm{Al,Ti:Al}} = {}^0L^{\mathrm{TiAl_3(l)}}_{\mathrm{Al:Al,Ti}} = -79752 + 26.614T$; ${}^0L^{\mathrm{TiAl_3(l)}}_{\mathrm{Al,Ti:Ti}} = {}^0L^{\mathrm{TiAl_3(l)}}_{\mathrm{Ti:Al,Ti}} = -118520$
TiAl2 (η)	${}^0G^{\mathrm{TiAl_2}}_{\mathrm{Al:Al}} = 15000 + 3{}^0G^{\mathrm{SER}}_{\mathrm{Al}}$; ${}^0G^{\mathrm{TiAl_2}}_{\mathrm{Ti:Ti}} = 15000 + 3{}^0G^{\mathrm{SER}}_{\mathrm{Ti}}$; ${}^0G^{\mathrm{TiAl_2}}_{\mathrm{Ti:Al}} = 2{}^0G^{\mathrm{SER}}_{\mathrm{Ti}} + {}^0G^{\mathrm{SER}}_{\mathrm{Al}}$; ${}^0G^{\mathrm{TiAl_2}}_{\mathrm{Al:Ti}} = 2{}^0G^{\mathrm{SER}}_{\mathrm{Al}} + {}^0G^{\mathrm{SER}}_{\mathrm{Ti}} - 117175 + 28.124T$; ${}^0L^{\mathrm{TiAl_2}}_{\mathrm{Al,Ti:Al}} = {}^0L^{\mathrm{TiAl_2}}_{\mathrm{Al:Al,Ti}} = -50997 + 14.098T$; ${}^0L^{\mathrm{TiAl_2}}_{\mathrm{Al,Ti:Ti}} = {}^0L^{\mathrm{TiAl_2}}_{\mathrm{Ti:Al,Ti}} = -65359 + 12.733T$
Ti2Al5 (ζ)	${}^0G^{\mathrm{Ti_2Al_5}}_{\mathrm{Al:Al}} = 60000 + 7{}^0G^{\mathrm{SER}}_{\mathrm{Al}}$; ${}^0G^{\mathrm{Ti_2Al_5}}_{\mathrm{Ti:Ti}} = 55000 + 7{}^0G^{\mathrm{SER}}_{\mathrm{Ti}}$; ${}^0G^{\mathrm{Ti_2Al_5}}_{\mathrm{Al:Ti}} = 5{}^0G^{\mathrm{SER}}_{\mathrm{Al}} + 2{}^0G^{\mathrm{SER}}_{\mathrm{Ti}} - 264790 + 67.463T$; ${}^0G^{\mathrm{Ti_2Al_5}}_{\mathrm{Ti:Al}} = 2{}^0G^{\mathrm{SER}}_{\mathrm{Al}} + 5{}^0G^{\mathrm{SER}}_{\mathrm{Ti}} + 987760$ ${}^0L^{\mathrm{Ti_2Al_5}}_{\mathrm{Al,Ti:Al}} = {}^0L^{\mathrm{Ti_2Al_5}}_{\mathrm{Al:Al,Ti}} = -108171$ ${}^0L^{\mathrm{Ti_2Al_5}}_{\mathrm{Al,Ti:Ti}}$ ${}^0L^{\mathrm{Ti_2Al_5}}_{\mathrm{Ti:Al,Ti}} = -232241 + 10.101T$
Ti_3Al_5	${}^0G^{\mathrm{Ti_3Al_5}}_{\mathrm{Al:Ti}} = 5{}^0G^{\mathrm{SER}}_{\mathrm{Al}} + 3{}^0G^{\mathrm{SER}}_{\mathrm{Ti}} - 311977 + 70.970T$

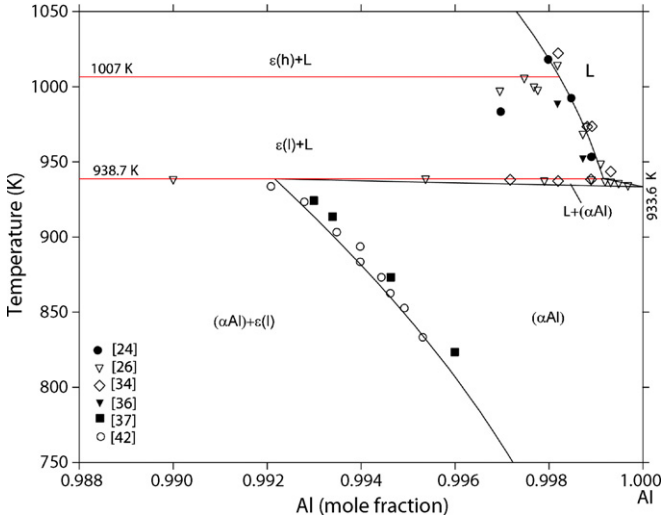

Fig. 5. Comparison of the calculated phase diagram in the Al-rich part of the Ti–Al system (lines) with experimental data of Refs. [24,26,34,36,37,42] (points).

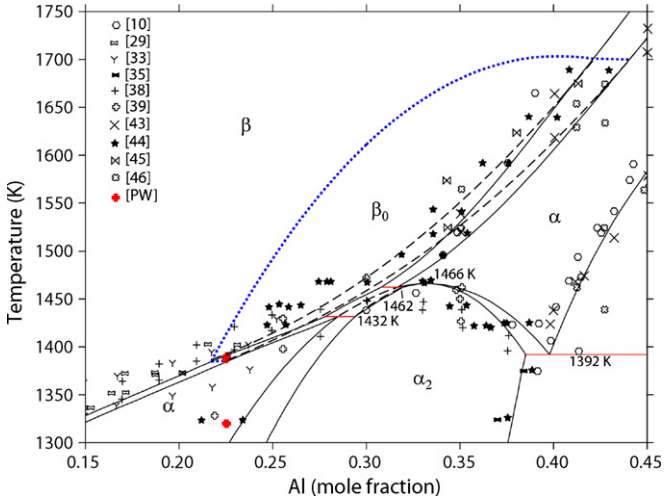

Fig. 6. Comparison of the calculated Ti-rich part of the Ti–Al system (lines) with experimental data of Refs. [10,29,33,35,38,39,43,44–46,PW] (points): dotted line represents the calculated A2 ↔ B2 second-order transition; dashed lines are the calculated α + β and β + α_2 boundaries without taking into consideration of the B2 ordering contribution. The invariant reactions $\beta_0 + \alpha_2 \leftrightarrow \alpha$ and $\beta_0 + \alpha \leftrightarrow \alpha_2$ occur when the B2 ordering is considered.

Table 4
The invariant reactions in the Al–Ti system

Reaction between phases $\phi_1/\phi_2/\phi_3$	Type	T (K)	Composition of Al in phases (at.%)			Comment/reference
			ϕ_1	ϕ_2	ϕ_3	
L ↔ β	Congruent	1983	8.5	8.5	–	[27]
		1962[a,b]	–	–		[PW]
		1963 ± 10	8.5 ± 3.5	8.5 ± 3.5	–	Assessment [14]
		1989	21.2	21.2	–	Description [9]
L ↔ β		**1963**	**9.6**	**9.6**	–	**Present description**
L + β ↔ α	Peritectic	1763	49.5	46.5	47.5	[43]
		1759	47.8	44.5	46.2	[67]
		1763	48	43.5	46	[68]
		1745	49.5–50.0	44.4–44.7	46.1–46.7	[29]
		1793	–	–	–	[69]
		1764	49.5	44.6	46.7	Assessment [14]
		1763	49.7	46.0	47.9	Description [8]
		1776	50.9	44.5	46	Description [9]
L+ β ↔ α		**1764**	**49.4**	**44.6**	**46.7**	**Present description**
L + α ↔ γ	Peritectic	1735	∼56	∼51	∼53	[43]
		1729[b]	–	–	–	[70,71]
		1737[c]	–	–	–	[27]
		∼1725	56.7	–	53.5	[41,72]
		∼1715	54.5–55.0	–	–	[67,73]
		1733	–	–	–	[74]
		–	–	51 ± 1	54 ± 1	[75]
		1723[d]	–	–	–	[PW]
		1729	59.0	50.5	54.5	Assessment [14]
		1736	54.9	51.7	54.7	Description [8]
		1717	56.4	50.2	54.1	Description [9]
L + α ↔ γ		**1729**	**54.7**	**51.5**	**54.6**	**Present description**
L + γ ↔ ζ or L + γ ↔ Ti_5Al_{11} or else L + $Ti_{1-x}Al_{1+x}$ ↔ Ti_5Al_{11}	Peritectic	1688	∼68	–	–	[40]
		1689	71.9	–	–	[11,15–17]
		1689	71.9	67.6	71.4	Description [8]
		1652	69.0	62.0	68.0	Description [9]
L + γ ↔ ζ		**1705**	**65.5**	**62.1**	**63.7**	**Present description**
L + ζ ↔ ε(h) or L + Ti_5Al_{11} ↔ ε(h) or else L + γ/1d-APS ↔ ε(h)	Peritectic	1683	–	–	–	[28]
		1668	∼79	71.4	75.0	[40]
		1660	81	71.1	75	[12,15–17,41]
		1681	–	–	–	[50]
		1698	78.0	71.5	75.0	[69]
		1698	78.0	71.5	75.0	[69]
		1678[e]	–	–	–	[PW]
		1685 ± 4	∼77.5	∼73	75	Assessment [14]
		1666	78.6	71.4	74.0	Description [8]
		1628	75.3	68.0	75.0	Description [9]
L + Ti_2Al_5 ↔ ε(h)		**1669**	**74.9**	**70.4**	**74.2**	**Present description**
Ti_5Al_{11} ↔ η or ζ ↔ η or else γ/1d-APS ↔ η	Congruent	1448	66.7	66.7	–	[40]
		1523	66.7	66.7	–	[88]
		1488	66.5	66.5	–	[15,16]
		1488	–	–	–	Assessment [11,13]
		1488	65.7	65.7	–	Assessment [14]
ζ ↔ η		**1497**	**66.6**	**66.6**	–	**Present description**
$Ti_{1-x}Al_{1+x}$ ↔ γ + η	Eutectoid	1443	∼63.3	∼62.3	∼65.8	[11,15,16]
ζ + γ ↔ η	Peritectoid	1478	71.4	60.0	66.7	[89]

Table 4 (*Continued*)

Reaction between phases $\phi_1/\phi_2/\phi_3$	Type	T (K)	Composition of Al in phases (at.%)			Comment/reference
			ϕ_1	ϕ_2	ϕ_3	
		1473	71.4	61.2	66.7	Description [8]
$Ti_5Al_{11} + \gamma \leftrightarrow \eta$	Peritectoid	1454	68.0	61.2	66.7	Description [9]
$\zeta \leftrightarrow \gamma + \eta$	**Eutectoid**	**1469**	**65.6**	**61.9**	**65.0**	**Present description**
$\alpha + \beta \leftrightarrow \alpha_2$	Peritectoid	~1473	35	~29	33	[39]
		1469	32	28.7	31.3	[76]
		1498	–	–	–	[35]
		1523	–	–	–	[77]
		1453	–	–	–	[78]
		1473 ± 10	33	~28	32	Assessment [14]
$\alpha \leftrightarrow \beta_0 + \alpha_2$	**Eutectoid**	**1462**	**31.7**	**30.8**	**32.0**	**Present description**
$\alpha \leftrightarrow \alpha_2$	Congruent	1442	32.5	32.5	–	[38]
		1437	30.9	30.9	–	Assessment [7,12]
		1439	31.0	31.0	–	Assessment [8,11]
		Absent				Assessment [14]
		1466	**0.333**	**0.333**	–	**Present description**
$\beta + \alpha_2 \leftrightarrow \alpha$	Peritectoid	1445 ± 8	23.9	28	26	[29]
		1453	18.7	26.0	21	[79]
		1373	15.5	25.3	23.5	[30]
		~1423	24	26	25	[39]
		1388	–	–	24	[35]
		1353 ± 20	15	22.5	17.5	[33]
		–	23.5	26	25	[44]
		1443 ± 10	25	~27.5	27	Assessment [14]
$\beta_0 + \alpha_2 \leftrightarrow \alpha$		**1432**	**27.8**	**29.4**	**28.5**	**Present description**
$\alpha \leftrightarrow \alpha_2 + \gamma$	Eutectoid	1393 ± 5	39	38.5	45.8	[80]
		1393 ± 10	39	38.5	45.8	[44]
		1383–1398	39.6	38.5	48.5	[81]
		1383	39	37.5	48	[38,43,82]
		1398	40	39	48	[41]
		1393 ± 10	39.0	38.5	46.5	Assessment [14]
		1387	39.2	37.7	47.8	Description [8]
		1384	40.5	39.3	48.2	Description [9]
$\alpha \leftrightarrow \alpha_2 + \gamma$		**1392**	**39.8**	**38.5**	**46.8**	**Present description**
γ/1d-APS $\leftrightarrow \eta + \varepsilon$(h) or $Ti_5Al_{11} \leftrightarrow \eta + \varepsilon$(h) or else $\zeta \leftrightarrow \eta + \varepsilon$(h)	Eutectoid	1263	70.2	66.7	75.1	[40]
		1248	–	–	–	[47,50]
		1253	–	–	–	[51]
		1268	–	–	–	[15,16]
		1243–1273	–	–	–	[41]
		1223	–	–	–	[88]
		1268	–	–	–	Assessment [11]
		1248–1253	71.5	67.0	74.2	Assessment [14]
		1265	71.4	66.7	73.6	Description [8]
		1260	68.0	66.7	75.0	Description [9]
$\zeta \leftrightarrow \eta + \varepsilon$(h)		**1249**	**69.8**	**67.3**	**74.8**	**Present description**
$\eta + \varepsilon$(h) $\leftrightarrow \varepsilon$(l)	Peritectoid	~1223	–	75	74.5	[15,16]
		~1223	–	–	–	Assessment [11,13,14]
$\eta + \varepsilon$(h) $\leftrightarrow \varepsilon$(l)		**1205**	**67.3**	**74.8**	**74.6**	**Present description**
$\gamma + \eta \leftrightarrow Ti_3Al_5$	Peritectoid	1083	~56	66.5	62	[11,15,16]
$\gamma + \eta \leftrightarrow Ti_3Al_5$		**1082**	**58.3**	**65.1**	**62.5**	**Present description**
ε(h) $\leftrightarrow \varepsilon$(l)	Allotropic	~911	–	–	–	[86]
		873–908	–	–	–	[87]
ε(h) $\leftrightarrow \varepsilon$(l) + L	Metatectic	1008	75	74.5	–	[15,16]
		1008	–	–	–	Assessment [11,13,14]

Table 4 (*Continued*)

Reaction between phases $\phi_1/\phi_2/\phi_3$	Type	T (K)	Composition of Al in phases (at.%)			Comment/reference
			ϕ_1	ϕ_2	ϕ_3	
$\varepsilon(h) \leftrightarrow \varepsilon(l) + L$		**1007**	**76.5**	**75.5**	**99.8**	**Present description**
$L + \varepsilon(l) \leftrightarrow (\alpha Al)$	Peritectic	938	99.9	75.0	99.3	[26,34,36,37,83–85]
		938	99.92	75.5	99.2	Assessment [14]
		938.2	99.8	75.1	99.2	Description [8]
		934.2	99.9	75.0	100	Description [9]
$L + \varepsilon(l) \leftrightarrow (\alpha Al)$		**938.7**	**99.9**	**75.7**	**99.2**	**Present description**

[a] The melting point for the alloy $Ti_{90}Al_{10}$ [PW].
[b] −26 K [14].
[c] −16 K [14].
[d] The melting point could be understated owing to as-cast state of sample.
[e] The melting point for the alloy $Ti_{26.5}Al_{73.5}$ [PW].

program Thermo-Calc [22] on the basis of the parameters obtained from the optimization described in Section 4.

5.1. Phase equilibria

The calculated phase diagram is presented in Fig. 3, with the temperatures of the invariant reactions being indicated. In Fig. 4 the calculated phase diagram and experimental data on phase equilibria from Refs. [10,24–51] as well as from the present work are plotted together for comparison. We conclude that the present description reproduces all experimental data within the limit of experimental uncertainties and note that a good agreement with the phase diagram most recently assessed by Schuster and Palm [14] is expectedly achieved.

In view of the fact that knowledge of precise Al–Ti phase equilibria in the Al-rich corner is important for the improvement of existing thermodynamic databases for Al-based alloys, special attention was focused on dilute Al–Ti alloys. The enlarged portion of the phase diagram for the composition range 98.8–100 at.% Al is presented in Fig. 5 and also shows good agreement with the experimental data of [24,26,34,36,42].

The phase diagram in the region affected by A2 ↔ B2 ordering is shown in Fig. 6. It should be mentioned here that Schuster and Palm considered the occurrence of B2 ordering at an Al content of about 25 at.% to be rather unlikely [14]. However, the existence of A2 ↔ B2 ordering in the ternary system Al–Nb–Ti was evidenced experimentally by several groups using TEM investigations [63–66] and was thermodynamically modelled by Servant and Ansara [23]. Therefore in the present work the data of [10] were selected for modelling the ordering phenomenon of the bcc β-phase in the binary Al–Ti system. Thus, the dotted line in Fig. 6 represents the calculated A2 ↔ B2 second-order transition according to the current thermodynamic description. The dashed lines are the calculated $\beta + \alpha$ and $\beta + \alpha_2$ boundaries without taking into consideration of the B2 ordering contribution. Obviously the invariant reactions $\beta_0 + \alpha_2 \leftrightarrow \alpha$ and $\beta_0 + \alpha \leftrightarrow \alpha_2$ occur when the B2 ordering is considered.

In Table 4 the temperature and the composition of coexisting phases are listed for each invariant reaction in the system and compared with available experimental and assessed data. There is a good agreement between the calculated and the experimental data. In order to fulfil Gibbs phase rule, the occurrence of the low temperature modification $\varepsilon(l)$ below the transition temperature reported by Braun and Ellner [15–17] ~1223 K for the Ti-rich phase boundary (74.5 at.% Al) and 1008 K for the Al-rich phase boundary (75 at.% Al), was modelled by two invariant reactions, i.e. peritectoid $\eta + \varepsilon(h) \leftrightarrow \varepsilon(l)$ and metatectic $\varepsilon(h) \leftrightarrow \varepsilon(l) + L$, respectively (see also Figs. 1a and 3). The temperatures of these reactions were calculated to be 1205 and 1007 K, respectively.

The present description takes into account the fact that all phases in the system are non-stoichiometric, except for Ti_3Al_5. For the Ti_3Al_5 phase experimental information concerning its stability is ambiguous. In the phase diagram of PW this phase is treated as stable, although the present authors, taking into consideration the critical assessment [14], do not exclude it to be metastable. In the latter case Ti_3Al_5 may be simply

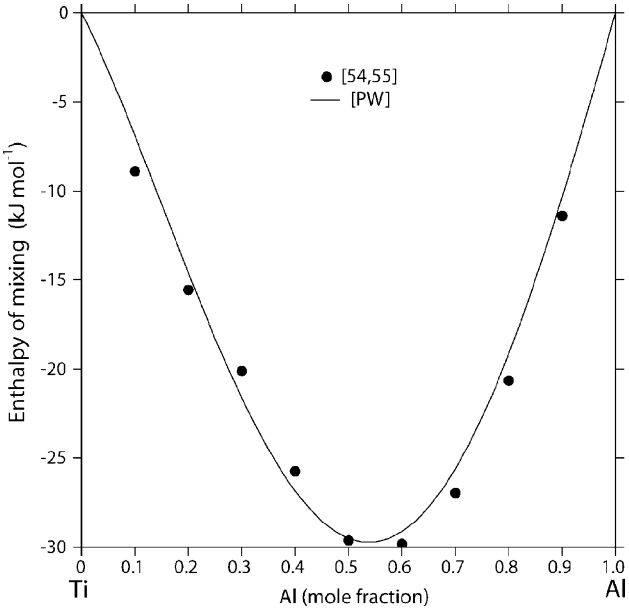

Fig. 7. Integral enthalpy of mixing of liquid Al–Ti alloys at 2000 K (reference state is liquid Al and liquid Ti): points are experimental calorimetric data of Refs. [54,55]; lines result from current thermodynamic description.

suspended because it practically has no effect on the γ(TiAl) phase boundary.

5.2. Thermodynamic properties

Fig. 7 shows the comparison of the calculated integral enthalpy of mixing of liquid alloys at 2000 K with experimental calorimetric data of Esin et al. [54,55]. The results are in very good agreement.

The comparison of the calculated integral enthalpy of formation of solid alloys at 298 and 1123 K with experimental data is shown in Fig. 8a and b, respectively. Fig. 9 depicts the integral Gibbs energy of formation of solid alloy at 850 K as function of composition. Again these figures demonstrate a quite reasonable agreement between the calculated and the experimentally measured data, though a somewhat larger difference can be observed in the fields related to the α_2 (Ti_3Al) phase. As mentioned by Zhang et al. [8] it is likely that in some experimental investigations the authors dealt with the disordered α (hcp_A3) phase instead of the ordered α_2 (Ti_3Al) phase. Thus, Kubaschewski et al. in their original work [52] identified the alloys obtained by direct synthesis calorimetry to be rather disordered α (hcp_A3). Due to this in Figs. 8 and 9 dashed lines show the results of calculations when suspending the α_2 (Ti_3Al) phase. In most cases when α_2 (Ti_3Al) was suspended, the agreement between calculated and experimental data improved.

The thermodynamic activity of the components in solid alloys of the Al–Ti system were investigated by several authors, using two different methods, i.e. electrochemical cell (EMF) and Knudsen effusion mass spectrometry (KEMS) [53,58–61]. Figs. 10 and 11 show the comparison of experimental and calculated values of the activity as functions of the reciprocal temperature for alloys with composition Ti–45 and Ti–62 at.% Al, respectively. The calculations were done both with the present thermodynamic description and with the one published in [8]. A reasonable agreement is achieved for the both alloys.

The most intensive measurement of thermodynamic activities of the components in solid alloys of this system was performed by Eckert et al. by means of direct measurements of the partial pressure of Al and Ti using KEMS at temperatures between 1170 and 1635 K [58,61]. This allowed also to evaluate the partial enthalpies and entropies of mixing for the solid (α, β, α_2 and

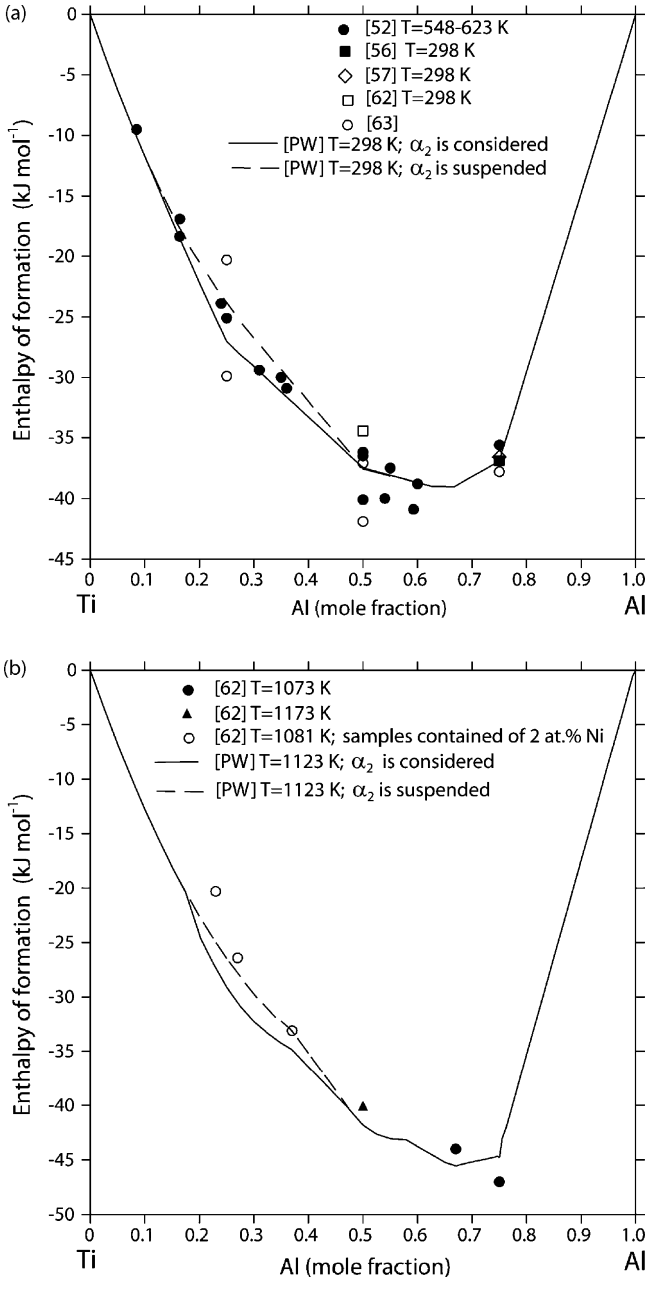

Fig. 8. Integral enthalpy of formation of solid Al–Ti alloys at 298 K (a) (reference state is fcc Al and hcp Ti) and 1123 K (b) (reference state is liquid Al and hcp Ti); points are experimental calorimetric data of Refs. [52,56,57,62,63]; lines result from current thermodynamic description.

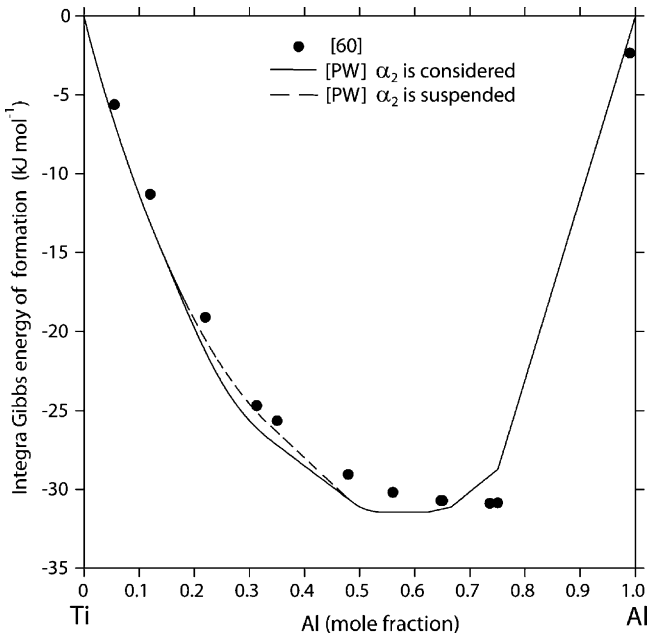

Fig. 9. Integral Gibbs energy of formation of solid Al–Ti alloys at 850 K (reference state is fcc Al and hcp Ti); points are experimental calorimetric data of Ref. [60]; lines result from current thermodynamic description.

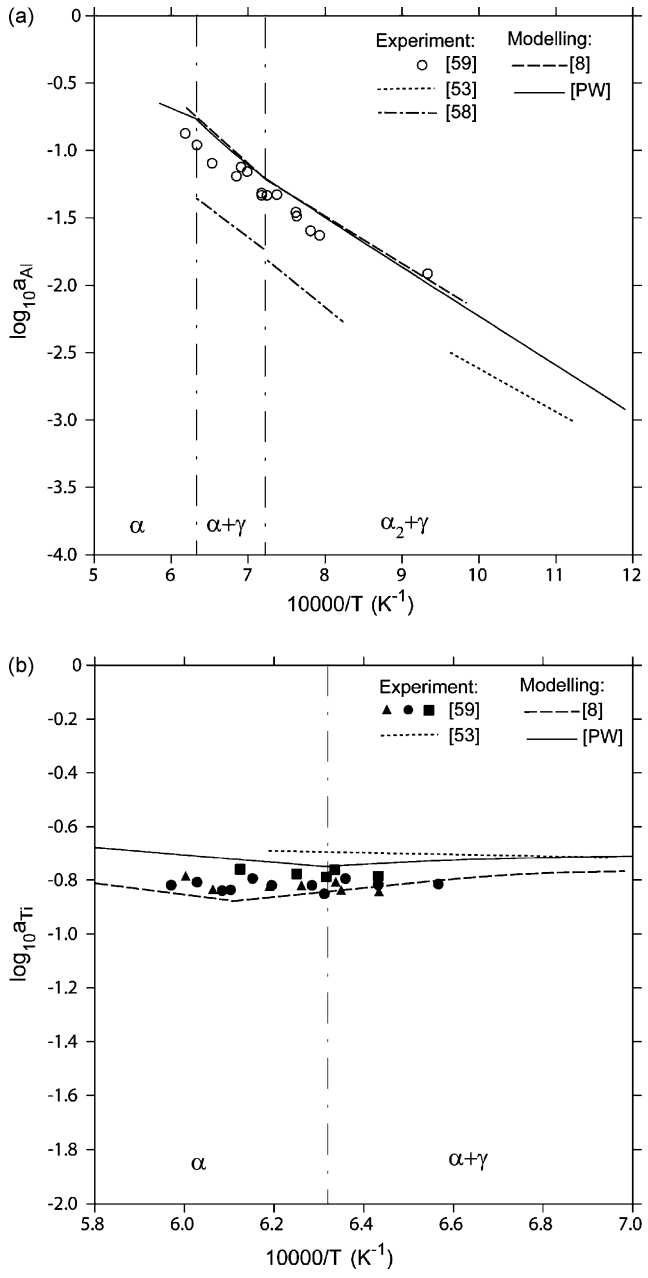

Fig. 10. Comparison between experimental [53,58,59] and calculated [8,PW] activities of Al (a) and Ti (b) in Ti–45 at.% Al; reference state is liquid Al and hcp Ti at the temperature of interest.

γ) alloys. Unfortunately, from these publications it is unclear to what reference state the obtained data are referred. The reference state for a component is important when dealing with activities, chemical potentials and enthalpies. Firstly, for each component of a system the data must be referred to a selected phase, temperature and pressure. Secondly, for all thermodynamic properties of all phases that contain this component, the same reference state must be used. Considering these arguments we have calculated the thermodynamic activities of the two components Al and Ti in the solid alloys for different reference states and compared them to the experimental data from Eckert et al. [58,61]. The results are given in Fig. 12 and they show that the experimentally measured activities of Ti are reproduced within the

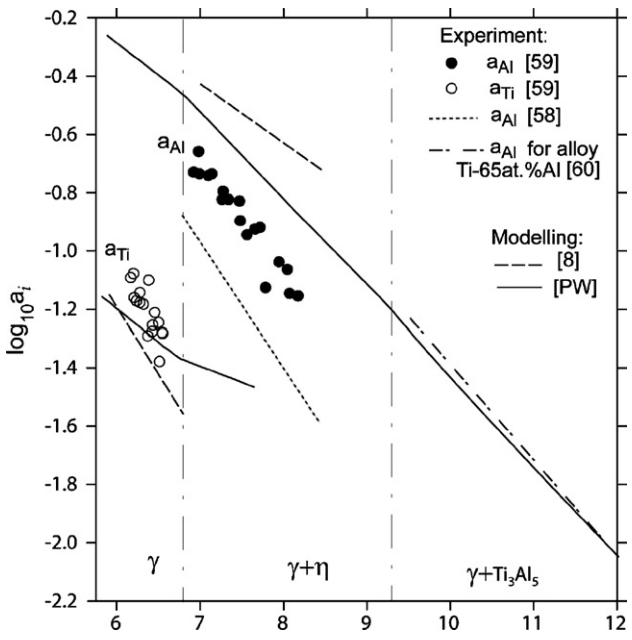

Fig. 11. Comparison between experimental [58–60] and calculated [8,PW] values for the activities of Ti and Al in Ti–62 at.% Al; reference state is liquid Al and hcp Ti at the temperature of interest.

limit of experimental errors when selecting the reference state for the component Ti to be the bcc_A2 phase at 1473 K. This choice seems reasonable, since at the given temperature Ti is stable just in the bcc_A2 crystal structure type. When calculating the activity of the component Al from the Ti data set using the Gibbs–Duhem equation, the calculated results do not fit to the experimental data set for Al irrespective of the selected reference state. This indicates that either the experimental method is not reliable for measuring Al vapour pressure or that the equation used to calculate the equilibrium partial pressure of pure Al (see Eq. (2) in Ref. [61]) is not valid at the temperature of the experiment (1473 K).

Summarizing, one may conclude that the present thermodynamic description of the Ti–Al system significantly better

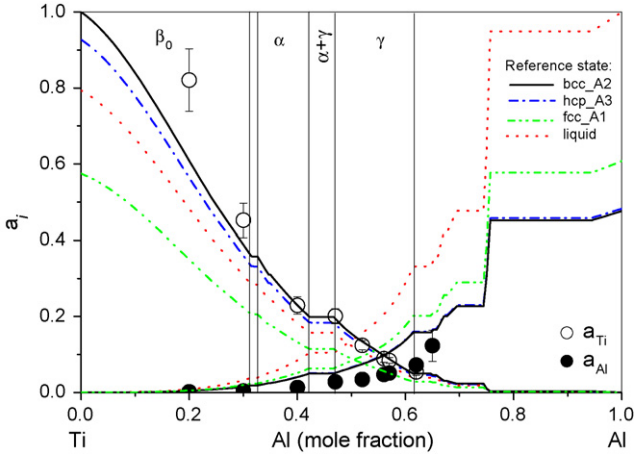

Fig. 12. Comparison between experimental [58,61] and calculated values for the activity of Ti and Al in the system Al–Ti at 1473 K for different reference states.

reproduces the majority of experimental data on phase equilibria and thermodynamic properties than earlier descriptions [3–10]. The advantage of the present description also relates to the simplicity of the selected models, which leads to significantly less quantity of parameters than in previous descriptions. This is convenient when attempting its integration into high-order systems, e.g. Al–B–Ti and Al–Nb–Ti, which will be discussed in following parts of this work.

Acknowledgements

The authors thank L.V. Artyukh, V.V. Garbuz, V.M. Petyukh and N.I. Tsyganenko for technical assistance and would like to express their gratitude for financial support from the Integrated Project IMPRESS, "Intermetallic Materials Processing in Relation to Earth and Space Solidification" (Contract NMP3-CT-2004-500635) co-funded by the European Commission in the Sixth Framework Programme and the European Space Agency (the Ti-rich portion) and from the WTL-project (Wissensbasierte technische Legierungen/knowledge-based technical alloys) under contract no. 223-21400204 funded by the Ministry of Sciences and Research, North-Rhine Westphalia, Germany (the Al-rich portion).

Appendix A

A.1. Thermodynamic database for the Al–Ti system

Appendix. Thermodynamic database for the Al-Ti system

```
ELEMENT /-   ELECTRON_GAS      0.0000E+00  0.0000E+00  0.0000E+00 !
ELEMENT VA   VACUUM            0.0000E+00  0.0000E+00  0.0000E+00 !
ELEMENT AL   FCC_A1            2.6982E+01  4.5773E+03  2.8322E+01 !
ELEMENT TI   HCP_A3            4.7880E+01  4.8240E+03  3.0720E+01 !

FUNCTION GHSERAL     298.15  -7976.15+137.093038*T-24.3671976*T*LN(T)
   -.001884662*T**2-8.77664E-07*T**3+74092*T**(-1);  7.00000E+02  Y
   -11276.24+223.048446*T-38.5844296*T*LN(T)+.018531982*T**2
   -5.764227E-06*T**3+74092*T**(-1);  9.33470E+02  Y
   -11278.378+188.684153*T-31.748192*T*LN(T)-1.230524E+28*T**(-9);
   2.90000E+03  N !
FUNCTION GHSERTI     298.15  -8059.921+133.615208*T-23.9933*T*LN(T)
   -.004777975*T**2+1.06716E-07*T**3+72636*T**(-1);  9.00000E+02  Y
   -7811.815+132.988068*T-23.9887*T*LN(T)-.0042033*T**2-9.0876E-08*T**3
   +42680*T**(-1);  1.15500E+03  Y
   +908.837+66.976538*T-14.9466*T*LN(T)-.0081465*T**2+2.02715E-07*T**3
   -1477660*T**(-1);  1.94100E+03  Y
   -124526.786+638.806871*T-87.2182461*T*LN(T)+.008204849*T**2
   -3.04747E-07*T**3+36699805*T**(-1);  4.00000E+03  N !
FUNCTION GLIQAL      298.15  +11005.029-11.841867*T+7.934E-20*T**7
   +GHSERAL#;  9.33470E+02  Y
   +10482.382-11.253974*T+1.231E+28*T**(-9)+GHSERAL#; 6000  N !
FUNCTION GLIQTI      298.15  +12194.415-6.980938*T+GHSERTI#;
   1.30000E+03  Y
   +368610.36-2620.99904*T+357.005867*T*LN(T)-.155262855*T**2
   +1.2254402E-05*T**3-65556856*T**(-1)+GHSERTI#;  1.94100E+03  Y
   +104639.72-340.070171*T+40.9282461*T*LN(T)-.008204849*T**2
   +3.04747E-07*T**3-36699805*T**(-1)+GHSERTI#; 6000  N !
FUNCTION GBCCAL      298.15  +10083-4.813*T+GHSERAL#;  6000   N !
FUNCTION GBCCTI      298.15  -1272.064+134.71418*T-25.5768*T*LN(T)
   -6.63845E-04*T**2-2.78803E-07*T**3+7208*T**(-1);  1.15500E+03  Y
    +6667.385+105.366379*T-22.3771*T*LN(T)+.00121707*T**2-8.4534E-07*T**3
   -2002750*T**(-1);  1.94100E+03  Y
    +26483.26-182.426471*T+19.0900905*T*LN(T)-.02200832*T**2
   +1.228863E-06*T**3+1400501*T**(-1);  4.00000E+03  N !
FUNCTION GFCCTI      298.15  +6000-.1*T+GHSERTI#;      6000   N !
FUNCTION GHCPAL      298.15  +5481-1.8*T+GHSERAL#;  6000   N !

TYPE_DEFINITION % SEQ *!
DEFINE_SYSTEM_DEFAULT ELEMENT 2 !
DEFAULT_COMMAND DEF_SYS_ELEMENT VA /- !

PHASE LIQUID:L %  1  1.0  !
CONSTITUENT LIQUID:L :AL,TI :  !
  PARAM G(LIQUID,AL;0)   298.15  +GLIQAL#;  6000   N  !
  PARAM G(LIQUID,TI;0)   298.15  +GLIQTI#;   6000   N  !
  PARAM G(LIQUID,AL,TI;0)   298.15 -118048+41.972*T; 6000   N  !
  PARAM G(LIQUID,AL,TI;1)   298.15 -23613+19.704*T;   6000   N  !
  PARAM G(LIQUID,AL,TI;2)   298.15  +34757-13.844*T;  6000   N  !

PHASE AL2TI  %  2 2   1 !
CONSTITUENT AL2TI  :AL,TI : AL,TI :  !
  PARAM G(AL2TI,AL:AL;0) 298.15  +15000+3*GHSERAL#;  6000  N  !
  PARAM G(AL2TI,TI:AL;0) 298.15  +GHSERAL#+2*GHSERTI#; 6000   N  !
  PARAM G(AL2TI,AL:TI;0) 298.15 -117175+28.124*T+2*GHSERAL#+GHSERTI#; 6000 N !
  PARAM G(AL2TI,TI:TI;0) 298.15  +15000+3*GHSERTI#;  6000  N  !
  PARAM G(AL2TI,AL,TI:AL;0)  298.15  -50997+14.098*T;  6000  N  !
  PARAM G(AL2TI,AL:AL,TI;0)  298.15  -50997+14.098*T;  6000  N  !
  PARAM G(AL2TI,TI:AL,TI;0)  298.15  -65359+12.733*T;   6000  N  !
  PARAM G(AL2TI,AL,TI:TI;0)  298.15  -65359+12.733*T;   6000  N  !

PHASE AL3TI_H  %  2 3   1 !
CONSTITUENT AL3TI_H  :AL,TI : AL,TI :  !
  PARAM G(AL3TI_H,AL:AL;0) 298.15  +80000+4*GHSERAL#;   6000   N  !
  PARAM G(AL3TI_H,TI:AL;0) 298.15  -72097+GHSERAL#+3*GHSERTI#; 6000 N !
  PARAM G(AL3TI_H,AL:TI;0) 298.15 -143733+35.088*T+3*GHSERAL#+GHSERTI#; 6000 N !
  PARAM G(AL3TI_H,TI:TI;0) 298.15  +80000+4*GHSERTI#;   6000   N  !
  PARAM G(AL3TI_H,AL,TI:AL;0)   298.15  -67583;  6000   N !
  PARAM G(AL3TI_H,AL:AL,TI;0)   298.15  -67583;  6000   N !
  PARAM G(AL3TI_H,TI:AL,TI;0)   298.15  -93086;  6000   N !
  PARAM G(AL3TI_H,AL,TI:TI;0)   298.15  -93086;  6000   N !

PHASE AL3TI_L  %  2 3   1 !
CONSTITUENT AL3TI_L  :AL,TI : AL,TI :  !
  PARAM G(AL3TI_L,AL:AL;0) 298.15 +80000+4*GHSERAL#;   6000   N  !
  PARAM G(AL3TI_L,TI:AL;0) 298.15 -53950+GHSERAL#+3*GHSERTI#; 6000 N !
  PARAM G(AL3TI_L,AL:TI;0) 298.15 -147620+38.395*T+3*GHSERAL#+GHSERTI#; 6000 N !
  PARAM G(AL3TI_L,TI:TI;0) 298.15  +80000+4*GHSERTI#;   6000   N  !
  PARAM G(AL3TI_L,AL,TI:AL;0)   298.15  -79752+26.614*T;  6000   N  !
  PARAM G(AL3TI_L,AL:AL,TI;0)   298.15  -79752+26.614*T;  6000   N  !
  PARAM G(AL3TI_L,TI:AL,TI;0)   298.15  -118520;  6000    N  !
  PARAM G(AL3TI_L,AL,TI:TI;0)   298.15  -118520;  6000    N  !

PHASE AL5TI2  %  2 5   2 !
CONSTITUENT AL5TI2  :AL,TI : AL,TI :  !
  PARAM G(AL5TI2,AL:AL;0) 298.15 +60000+7*GHSERAL#;  6000    N  !
  PARAM G(AL5TI2,TI:AL;0) 298.15 +987760+2*GHSERAL#+5*GHSERTI#; 6000   N  !
  PARAM G(AL5TI2,AL:TI;0) 298.15 -264790+67.463*T+5*GHSERAL#+2*GHSERTI#; 6000 N !
  PARAM G(AL5TI2,TI:TI;0) 298.15  +55000+7*GHSERTI#; 6000 N  !
  PARAM G(AL5TI2,AL,TI:AL;0)   298.15  -108171;  6000    N  !
  PARAM G(AL5TI2,AL:AL,TI;0)   298.15  -108171;  6000    N  !
  PARAM G(AL5TI2,TI:AL,TI;0)   298.15  -232241+10.101*T;  6000  N  !
  PARAM G(AL5TI2,AL,TI:TI;0)   298.15  -232241+10.101*T;  6000  N  !

PHASE AL5TI3  %  2 5   3 !
CONSTITUENT AL5TI3  :AL : TI :  !
  PARAM G(AL5TI3,AL:TI;0) 298.15 -311977+70.970*T+5*GHSERAL#+3*GHSERTI#; 6000 N !

TYPE_DEFINITION & GES A_P_D ALTI MAGNETIC  -1.0    4.00000E-01 !
PHASE ALTI  %&  2 1   1 !
CONSTITUENT ALTI  :AL%,TI : AL,TI% :  !
  PARAM G(ALTI,AL:AL;0)   298.15  +2*GHSERAL#+4;  6000   N    !
  PARAM G(ALTI,TI:AL;0)   298.15  -81008+14.722*T+GHSERAL#+GFCCTI#;  6000   N  !
  PARAM G(ALTI,AL:TI;0)   298.15  -81008+14.722*T+GHSERAL#+GFCCTI#;  6000   N  !
  PARAM G(ALTI,TI:TI;0)   298.15  +2*GFCCTI#;  6000   N    !
  PARAM G(ALTI,AL,TI:AL;0)   298.15  -88993+41.695*T;  6000    N  !
  PARAM G(ALTI,AL:AL,TI;0)   298.15  -88993+41.695*T;  6000    N  !
  PARAM G(ALTI,AL,TI:AL;1)   298.15  +27363;  6000   N  !
  PARAM G(ALTI,AL:AL,TI;1)   298.15  +27363;  6000   N  !
  PARAM G(ALTI,AL,TI:AL;2)   298.15  +42189;  6000   N  !
  PARAM G(ALTI,AL:AL,TI;2)   298.15  +42189;  6000   N  !
  PARAM G(ALTI,TI:AL,TI;0)   298.15  -31963+6.952*T;  6000    N  !
  PARAM G(ALTI,AL,TI:TI;0)   298.15  -31963+6.952*T;  6000    N  !

TYPE_DEFINITION ' GES A_P_D ALTI3_D019 MAGNETIC  -3.0    2.80000E-01 !
PHASE ALTI3_D019  %'  2 3   1 !
  CONSTITUENT ALTI3_D019  :AL,TI : AL,TI :  !

  PARAM G(ALTI3_D019,AL:AL;0) 298.15 +4*GHCPAL#;  6000   N  !
  PARAM G(ALTI3_D019,TI:AL;0) 298.15 -113676+20.833*T+GHCPAL#+3*GHSERTI#; 6000 N !
  PARAM G(ALTI3_D019,AL:TI;0) 298.15 -16443+5.4*T+3*GHCPAL#+GHSERTI#; 6000 N  !
```

```
 PARAM G(ALTI3_D019,TI:TI;0) 298.15  +20+4*GHSERTI#;        6000  N  !
 PARAM G(ALTI3_D019,AL,TI:AL;0) 298.15  -269912+86.338*T;  6000  N  !
 PARAM G(ALTI3_D019,TI:AL,TI;0) 298.15  -13704+5.318*T;     6000  N  !

TYPE_DEFINITION ( GES A_P_D BCC_A2 MAGNETIC  -1.0    4.00000E-01 !
PHASE BCC_A2  %(  2 1   3 !
CONSTITUENT BCC_A2  :AL,TI : VA :  !
 PARAM G(BCC_A2,AL:VA;0)  298.15  +GBCCAL#;  6000  N    !
 PARAM G(BCC_A2,TI:VA;0)  2.98140E+02  +GBCCTI#;  4000  N  !
 PARAM G(BCC_A2,AL,TI:VA;0)  298.15  -132903+39.961*T;  6000    N  !
 PARAM G(BCC_A2,AL,TI:VA;1)  298.15  +4890;  6000    N  !
 PARAM G(BCC_A2,AL,TI:VA;2)  298.15  +400;   6000    N  !

TYPE_DEFINITION / GES AMEND_PHASE_DESCRIPTION BCC_B2 DIS_PART BCC_A2,,,!
TYPE_DEFINITION M GES AMEND_PHASE_DESCRIPTION BCC_B2 C_S 2 AL AL:TI:VA: !
PHASE BCC_B2  / M  3 .5   .5   3 !
CONSTITUENT BCC_B2  :AL,TI : AL,TI : VA :  !
 PARAM G(BCC_B2,TI:AL:VA;0)  298.15  -17501;   6000  N    !
 PARAM G(BCC_B2,AL:TI:VA;0)  298.15  -17501;   6000  N    !
 PARAM G(BCC_B2,AL,TI:AL:VA;0)  298.15  +6155;  6000  N  !
 PARAM G(BCC_B2,AL:AL,TI:VA;0)  298.15  +6155;  6000  N  !
 PARAM G(BCC_B2,AL,TI:AL:VA;1)  298.15  +6292;  6000  N  !
 PARAM G(BCC_B2,AL:AL,TI:VA;1)  298.15  +6292;  6000  N  !
 PARAM G(BCC_B2,TI:AL,TI:VA;0)  298.15  -21406;  6000  N  !
 PARAM G(BCC_B2,AL,TI:TI:VA;0)  298.15  -21406;  6000  N  !
 PARAM G(BCC_B2,TI:AL,TI:VA;1)  298.15  -1080;   6000  N  !
 PARAM G(BCC_B2,AL,TI:TI:VA;1)  298.15  -1080;   6000  N  !

TYPE_DEFINITION * GES A_P_D FCC_A1 MAGNETIC  -3.0    2.80000E-01 !
PHASE FCC_A1  %*  2 1   1 !
CONSTITUENT FCC_A1  :AL,TI : VA :  !
 PARAM G(FCC_A1,AL:VA;0)  298.15  +GHSERAL#;  6000  N    !
 PARAM G(FCC_A1,TI:VA;0)  298.15  +6000-.1*T+GHSERTI#; 6000  N  !
 PARAM G(FCC_A1,AL,TI:VA;0)  298.15  -119185+40.723*T; 6000  N  !

TYPE_DEFINITION + GES A_P_D HCP_A3 MAGNETIC  -3.0    2.80000E-01 !
PHASE HCP_A3  %+  2 1   .5 !
CONSTITUENT HCP_A3  :AL,TI : VA :  !
 PARAM G(HCP_A3,AL:VA;0) 298.15  +GHCPAL#;  6000  N  !
 PARAM G(HCP_A3,TI:VA;0) 2.98140E+02  +GHSERTI#;  4000  N  !
 PARAM G(HCP_A3,AL,TI:VA;0)  298.15  -134164+37.863*T;  6000  N  !
 PARAM G(HCP_A3,AL,TI:VA;1)  298.15  -3475+0.825*T;  6000    N  !
 PARAM G(HCP_A3,AL,TI:VA;2)  298.15  -7756;  6000    N  !
```

References

[1] V.T. Witusiewicz, A.A. Bondar, U. Hecht, S. Rex, T.Ya. Velikanova, J. Alloys Compd. 448 (2008) 185–194.
[2] V.T. Witusiewicz, A.A. Bondar, U. Hecht, S. Rex, T.Ya. Velikanova, J. Alloys Compd. 456 (2008) 143–150.
[3] L. Kaufman, H. Nesor, CALPHAD 2 (1978) 325–348.
[4] W.W. Liang, CALPHAD 7 (1983) 13–20.
[5] J.L. Murray (Ed.), Phase Diagrams of Binary Titanium Alloys, ASM International, Metals Park, OH, 1987.
[6] J.L. Murray, Metall. Trans. A 19A (1988) 243–247.
[7] U.R. Kattner, J.-C. Lin, Y.A. Chang, Metall. Trans. A 23A (1992) 2081–2090.
[8] F. Zhang, S.L. Chen, Y.A. Chang, U.R. Kattner, Intermetallics 5 (1997) 471–482.
[9] N. Saunders, Al–Ti system, in: I. Ansara, A.T. Dinsdale, M.H. Rand (Eds.), COST 507: Thermochemical Database for Light Metal Alloys, vol. 2, European Communities, Brussels, 1998.
[10] I. Ohnuma, Y. Fujita, H. Mitsui, K. Ishikava, R. Kainuma, K. Ishida, Acta Mater. 48 (2000) 3113–3123.
[11] A. Grytsiv, P. Rogl, H. Schmidt, G. Giester, J. Phase Equilib. 24 (2003) 511–527.
[12] R. Schmid-Fetzer, "Al–Ti (Aluminium–Titanium)", MSIT Binary Evaluation Program, MSI, Stuttgart, 2003, p. 22.
[13] V. Raghavan, J. Phase Equilib. Diffus. 26 (2005) 171–172.
[14] J.C. Schuster, M. Palm, J. Phase Equilib. Diffus. 27 (2006) 255–277.
[15] J. Braun, Strukturelle und konstitutionelle Untersuchungen an intermetallischen Phasen im System Ti–Al, PhD Thesis, Max-Planck-Institut für Metallforschumg, Stuttgart, 1999, pp. 1–283 (in German).
[16] J. Braun, M. Ellner, Z. Metallkd. 91 (2000) 389–392 (in German).
[17] J. Braun, M. Ellner, Metall. Mater. Trans. A 32A (2001) 1037–1048.
[18] T.B. Massalski, P.R. Subramanian, H. Okomoto, L. Kasprzak (Eds.), Binary Alloy Phase Diagrams, vol. 3, 2nd ed., ASM International, Metals Park, OH, 1990.
[19] A.T. Dinsdale, CALPHAD 15 (1991) 317–425.
[20] O. Redlich, A.T. Kister, Ind. Eng. Chem. 40 (1948) 345–348.
[21] M. Hillert, L.-I. Staffansson, Acta Chem. Scand. 24 (1970) 3618–3626.
[22] B. Sundman, B. Jansson, J.-O. Andersson, CALPHAD 9 (1985) 153–190.
[23] C. Servant, I. Ansara, Ber. Bunsenges. Phys. Chem. 102 (1998) 1189–1205.
[24] E. van Erckelens, Metall. Erz 20 (11) (1923) 206–210 (in German).
[25] W. Manchot, A. Leber, Z. Anorg. Allg. Chem. 150 (1926) 26–34 (in German).
[26] W.L. Fink, K.R. van Horn, P.M. Budge, Trans. AIME 93 (1931) 421–439.
[27] H.R. Ogden, D.J. Maykuth, W.L. Finlay, R.I. Jaffee, J. Met. 3 (1951) 1150–1155.
[28] I.I. Kornilov, E.N. Pylaeva, M.A. Volkova, Izv. Akad. Nauk. SSSR, Otd. Khim. Nauk 7 (1956) 771–778 (in Russian).
[29] E. Ence, H. Margolin, Trans. Metall. Soc. AIME 221 (1961) 151–157.
[30] D. Clark, K.S. Jepson, G.I. Lewis, J. Inst. Met. 91 (1962/1963) 197–203.
[31] M.J. Blackburn, Trans. Met. Soc. AIME 239 (1967) 1200–1208.
[32] G. Lütjering, S. Weissmann, Acta Metall. 18 (1970) 785–795.
[33] I.I. Kornilov, T.T. Nartova, S.P. Chernyshova, Izv. Akad. Nauk SSSR, Met. 6 (1976) 92–198 (in Russian).
[34] K. Shibata, T. Sato, G. Ohira, J. Cryst. Growth 44 (1978) 435–445.
[35] K. Ouchi, Y. Iijima, K. Hirano, in: H. Kimura, O. Izumi (Eds.), Titanium'80—Science and Technology, vol. 1, TMS, 1980, pp. 559–568.
[36] A. Abdel-Hamid, C.H. Allibert, F. Durand, Z. Metallkd. 75 (1984) 455–458.
[37] S. Hori, H. Tai, E. Matsumoto, J. Jpn. Inst. Light Met. 34 (1984) 377–381.
[38] R.D. Shull, A.J. McAlister, R.C. Reno, in: G. Lütjering, U. Zwicker, W. Bunk (Eds.), Titanium—Science and Technology, vol. 3, DGM, Oberursel, FRG, 1985, pp. 1459–1466.
[39] R.M. Waterstrat, Effect of interstitial elements on phase relationships in the titanium–aluminum system, NISTIR 88-3856, US Dept. of Commerce, 1988, pp. 1–53.
[40] K. Kaltenbach, S. Gama, D.G. Pinatti, K. Schulze, Z. Metallkd. 80 (1989) 511–514 (in German).
[41] J.C. Schuster, H. Ipser, Z. Metallkd. 81 (1990) 389–396 (in German).
[42] Y. Minamino, T. Yamane, H. Araki, N. Takeuchi, Metall. Trans. 22A (1991) 783–786.
[43] J.H. Perepezko, J.C. Mishurda, in: F.H. Froes, I. Caplan (Eds.), Titanium'92—Science and Technology, vol. 1, TMS, 1993, pp. 563–570.
[44] R. Kainuma, M. Palm, G. Inden, Intermetallics 2 (1994) 321–332.
[45] J.J. Ding, G.W. Qin, S.M. Hao, X.T. Wang, G.L. Chen, J. Phase Equilib. 17 (1996) 117–120.
[46] D. Veeraraghavan, U. Pilchowski, B. Natarajan, V.K. Vasudevan, Acta Mater. 46 (1998) 405–421.
[47] M. Palm, F. Stein, in: Y.W. Kim, D.M. Dimiduk, M.H. Loretto (Eds.), Gamma Titanium Aluminides 1999, TMS, 1999, pp. 161–168.
[48] I.S. Jung, M.C. Kim, J.H. Lee, M.H. Oh, D.M. Wee, Intermetallics 7 (1999) 1247–1253.
[49] F. Stein, M. Palm, in: D.G. Morris, S. Naka, P. Caron (Eds.), Proc. Euromat'99, Vol. 10, Wiley–VCH, Weinheim, Germany, 2000, pp. 336–344.
[50] M. Palm, L.C. Zhang, F. Stein, G. Sauthoff, Intermetallics 10 (2002) 523–540.
[51] R. Kainuma, J. Sato, I. Ohnuma, K. Ishida, Intermetallics 13 (2005) 784–791.
[52] O. Kubaschewski, W.A. Dench, Acta Metall. 3 (1955) 339–346.
[53] V.V. Samokhval, P.A. Poleshchuk, A.A. Vecher, Zh. Fiz. Khim. 45 (1971) 2071–2078 (in Russian).
[54] Yu.O. Esin, N.P. Bobrov, M.S. Petrushevskiy, P.V. Gel'd, Izv. Akad.Nauk SSR, Met. 5 (1974) 104–109 (in Russian).
[55] Yu.O. Esin, N.P. Bobrov, M.S. Petrushevskii, P.V. Gel'd, Tepl. Vys. Temp. 13 (1975) 84–88 (in Russian).
[56] J.M. Stuve and M.J. Ferrante, US Bur. Mines, Rep. Invest. #7834, Washington, DC, 1974, pp. 1–9.
[57] S.V. Meschel, O.J. Kleppa, in: J.S. Faulkner, R.G. Jordan (Eds.), Metallic Alloys, Experimental and Theoretical Perspectives, Kluwer Academic, The Netherlands, 1994, pp. 103–112.
[58] M. Eckert, L. Bencze, D. Kath, H. Nickel, K. Hilpert, Ber. Bunsenges. Phys. Chem. 100 (1996) 418–424.
[59] N.S. Jacobson, M.P. Brady, G.M. Mehrotra, Oxid. Met. 52 (1999) 537–556.
[60] R.G. Reddy, A.M. Yahya, L. Brewer, J. Alloys Compd. 321 (2001) 223–227.

[61] M. Eckert, D. Kath, K. Hilpert, Metall. Met. Trans. 30A (1999) 1315–1999.
[62] M. Nassik, F.Z. Chrifi-Alaoui, K. Mahdouk, J.C. Gachon, J. Alloys Compd. 350 (2003) 151–154.
[63] K. Rzyman, Z. Moser, J.C. Gachon, Pol. Arch. Met. Mater. 49 (2004) 545–563.
[64] M.J. Kaufman, T.F. Broderick, C.H. Ward, J.K. Kim, R.G. Rowe, F.H. Froes, in: P. Lacombe, R. Tricot, G. Baranges (Eds.), Proceedings of the 6th Word Conference on Titanium, Part II, Les Ulis, France, 1988, p. 985.
[65] D. Benerjee, T.K. Nandy, A.K. Gogia, K. Muraleedharan, in: P. Lacombe, R. Tricot, G. Baranges (Eds.), Proceedings of the 6th Word Conference on Titanium, Part II, Les Ulis, France, 1988, p. 1091.
[66] A. Hellwig, M. Palm, G. Inden, Intermetallics 6 (1998) 79–84.
[67] E.L. Hall, S.C. Huang, Acta Metall. Mater. 38 (1990) 539–549.
[68] Yu. Kovneristy, P.B. Budberg, in: I.V. Gorynin, S.S. Ushkov (Eds.), Titanium'99—Science and Technology, Part 1, Prometey, St. Petersburg, Russia, 2000, pp. 115–123.
[69] M. Bulanova, L. Tretyachenko, M. Golovkova, K. Meleshevich, J. Phase Equilib. 25 (2004) 209–229.
[70] C.D. Anderson, Phase Stability, Metastability, and Solidification Kinetics in Binary Ti–Al, PhD Thesis, Vanderbilt University, Nashville, TN, 1991, pp. 1–165 (cited after [14]).
[71] C.D. Anderson, W.H. Hofmeister, R.J. Bayuzick, Metall. Trans. 24A (1993) 61–66.
[72] P.A. Farrar, H. Margolin, Air Force Materials Lab. Tech. Rept. AFML-TR-65-69, 1965 (cited after [14]).
[73] S.C. Huang, P.A. Siemers, Metall. Trans. 20A (1989) 1899–1906.
[74] D.J. McPherson, M. Hansen, Z. Metallkd. 45 (1954) 76–82 (in German).
[75] D.B. Snow, C.T. Burilla, B.F. Oliver, in: F.H. Froes, I. Caplan (Eds.), Titanium'92—Science and Technology, vol. 2, TMS, 1993, pp. 1091–1098.
[76] A. Suzuki, M. Takeyama, T. Matsuo, Intermetallics 10 (2002) 915–924.
[77] I.I. Kornilov, E.N. Pylaeva, M.A. Volkova, P.I. Kripyakevich, V.Y. Markiv, Dokl. Akad. Nauk. SSSR 161 (1965) 843–846 (in Russian).
[78] P.L. Martin, H.A. Lipsitt, N.T. Nuhfer, J.C. Williams, in: H. Kimura, O. Izumi (Eds.), Titanium'80—Science and Technology, vol. 2, TMS, 1980, pp. 1245–1254.
[79] H. Sasano, T. Tsujimoto, in: R.I. Jaffee, H.M. Burte (Eds.), Titanium—Science and Technology, vol. 3, Plenum Press, New York, 1973, pp. 1635–1647.
[80] A. Hellwig, G. Inden, M. Palm, Scripta Metall. Mater. 27 (1992) 143–148.
[81] A. Bartz, L. Rothenflue, M. Saqib, R. Omlor, H.A. Lipsitt, in: F.H. Froes, I. Caplan (Eds.), Titanium'92—Science and Technology, vol. 2, TMS, 1993, pp. 1291–1298.
[82] J.C. Mishurda, J.C. Lin, Y.A. Chang, J.H. Perepezko, MRS Symp. Proc. 133 (1989) 57–62.
[83] J. Cisse, H.W. Kerr, G.F. Bolling, Metall. Trans. 5 (1974) 633–641.
[84] H.W. Kerr, J. Cisse, G.F. Bolling, Acta Metall. 22 (1974) 677–686.
[85] H. Nishimura, E. Matsumoto, Nippon Kinzoku Gakkaishi 4 (1940) 339–343 (in Japanese).
[86] F.J.J. van Loo, G.D. Rieck, Acta Metall. 21 (1973) 61–71.
[87] V.B. Rao, C.R. Houska, Metall. Trans. 14A (1983) 61–66.
[88] A. Raman, K. Schubert, Z. Metallkd. 56 (1965) 44–52 (in German).
[89] J.C. Mishurda, J.H. Perepezko, in: Y.W. Kim, R.R. Boyer (Eds.), Microstructure/Property Relationships in Titanium Aluminides and Alloys, TMS, 1991, pp. 3–30.